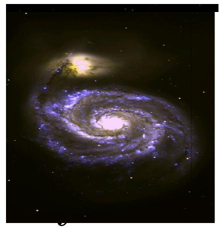

"Abundances of Elements in Nebulae and Chemical Evolution of the Universe"

S.N. Nahar, M. Dance, E. Palay, A.K. Pradhan
Astronomy, The Ohio State University
Columbus, Ohio
Email: nahar@astronomy.ohio-state.edu
web: http://www.astronomy.ohio-state.edu/∼nahar

APS April Meeting 2013
Denver, Colorado
April 13-16, 2013
*Support: DOE, NSF, Ohio Supercomputer Center

INTRODUCTION

- **I will discuss about infrared to optical photons from ionized gaseous nebulae**
- **These nebulae are assoicated with the birth of stars and the end point of stellar evolution**
- **Their elemental abundances, chemical enrichment are therefore related to chronometer of the life ot the universie itself**
- **Radiation from Ultra-Luminus infrared galaxy (ULIRG) gives the information of the cheimcal evolution of the universe**
- **Will present stduy of Ne V lines as detected from these objects**

Abundance of Elements Orion Nebula - Birthplace of Stars

[Composed by images from Spitzer & Hubble]

- $\sim$ 1500 Lyr away, closest cosmic cloud to us
- Center bright & yellow gas - illuminated ultraviolet (UV) radiation

Images: Spitzer - Infrared (red & orange) C rich molecules - hydrocarbons, Hubble - optical & UV (swirl green) of H, S

- Small dots - infant stars; over 1000 young stars
- Shows low ionization lines of C, N, O, Ne, Fe

Abundance of Elements

PLANETARY NEBULAE - Endpoint of a Star

PNe: Final stage of a Star [PNe K 4-55 below]

- **Condensed central star: very high T $\sim$ 100,000 K ($>>$ T $\leq$ 40,000 K - typical star)**
- **Envelope: thin gas radiatively ejected & illuminated by central star radiation: red (N), blue (O)**
- **Lines of low ionization states - low ρ & low T**

Ultra Luminus Infrared Galaxy (ULIRG)

ULIRG: IRAS-19297-0406

- **ULIRG - emits more than 10^{11} solar luminosities in IR (as stars are born), heavily dust obscured**
- **Only far-infrared photons escape from absorption and are observed at high redshift (by SPITZER, HERSCHEL, SOFIA) which provides information on chemical evolution of the galaxy.**

ELECTRON-IMPACT EXCITATION (EIE)

The most common source of these radiation is collsion:

$$\mathbf{e} + \mathbf{X}^{+\mathbf{Z}} \rightarrow \mathbf{e}' + \mathbf{X}^{+\mathbf{Z}*} \rightarrow \mathbf{e}' + \mathbf{X}^{+\mathbf{Z}} + \mathbf{h}\nu$$

ii) Via Autoionization (AI) (2-steps):

$$\epsilon + \mathbf{X}^{+\mathbf{Z}} \rightleftharpoons (\mathbf{X}^{+\mathbf{Z-1}})^{**} \rightleftharpoons \begin{cases} \epsilon + \mathbf{X}^{+\mathbf{Z}} & \text{AI} \\ X^{+Z-1} + h\nu & \text{DR} \end{cases}$$

AI state $[(\mathbf{X}^{+\mathbf{Z-1}})^{**}]$ (10^{14}/s) results in a resonance

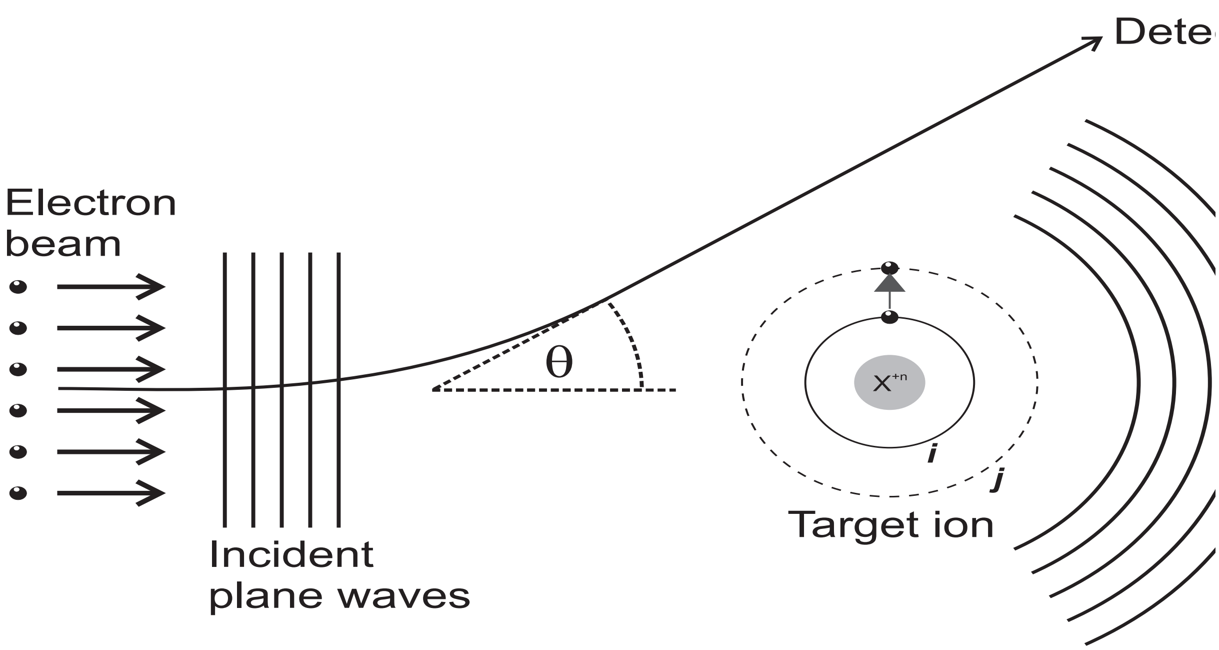

- **- A photon emits as the excitation decays**
- forms a diagnostic, often forbidden, emission line
- the scattered electron shows features with energy
- **Atomic quantity:** ***Collision Strength (Ω)***
- **Common in low T, low ρ astrophysical plasmas, such as, in Orion Nebula, Planetary Nebulae (PNe)**

EIE: Infrared Lines of Ne V

Ne V transitions (forbidden) in the lowest levels of ground configuration: $1s^2 2s^2 2p^2$ ($^3P_{0,1,2}, ^1D_2, ^1S_0$)

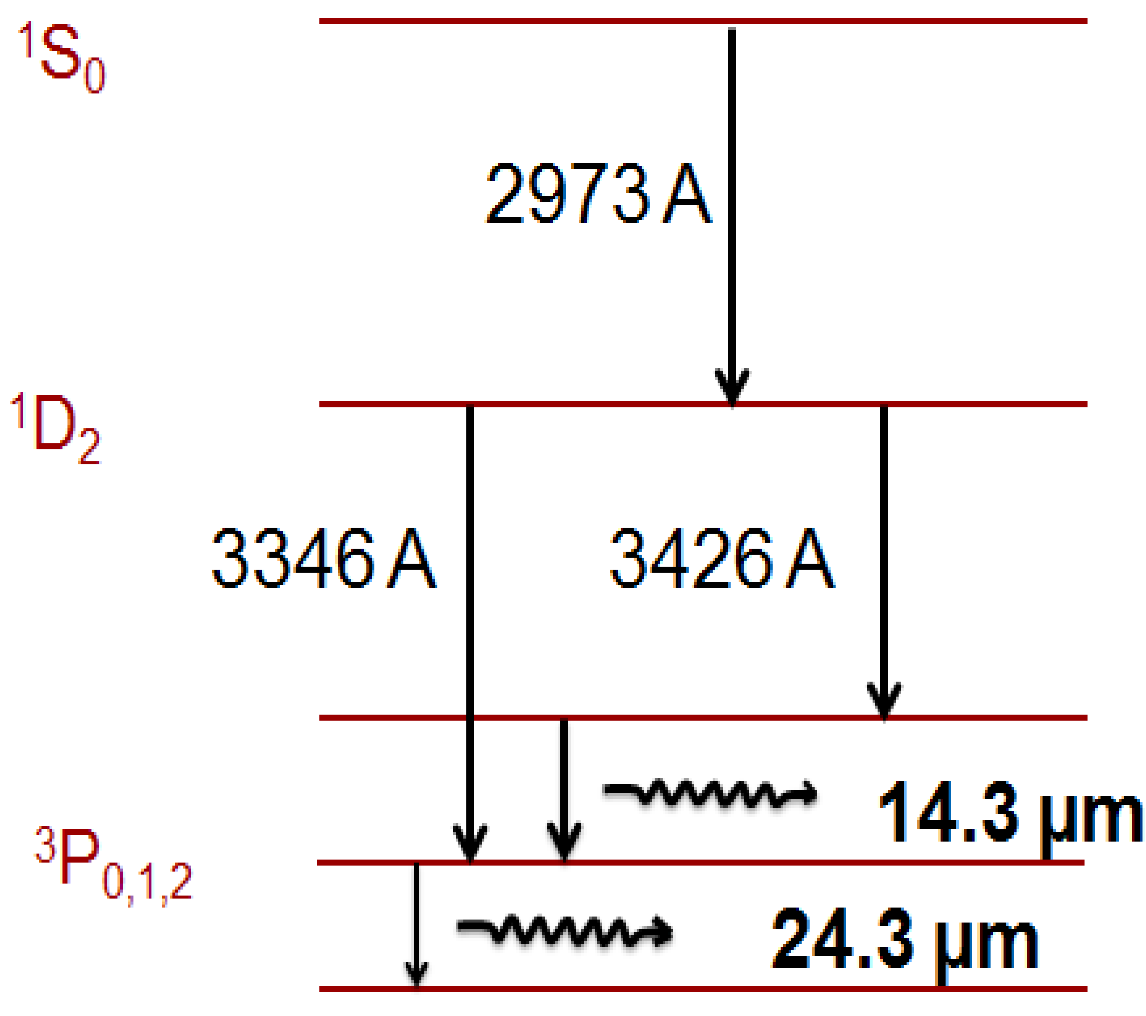

- **Collisionally Excited Lines (CEL):**

$$e + X^{+} \rightarrow X^{+*} \rightarrow X^{+} + h\nu$$

Determination of Abundance:

- The intensity of a CEL of ion X_i

$$\mathbf{I_{ba}(X_i, \lambda_{ba}) = \left[\frac{h\nu}{4\pi} n_e n_{ion}\right] q_{ba}} \tag{1}$$

$\mathbf{q_{ba}}$ - EIE rate coeffcient in cm^3/sec.

The abundance, $\mathbf{n(X)/n(H)}$ with respect to H

$$\mathbf{I(X_i, \lambda_{ba}) = \left[\frac{h\nu}{4\pi} A_{ba} \frac{N(b)}{\Sigma_j N_j(X_i)} \frac{n(X_i)}{n(X)}\right] \left[\frac{n(X)}{n(H)}\right] n(H)}$$

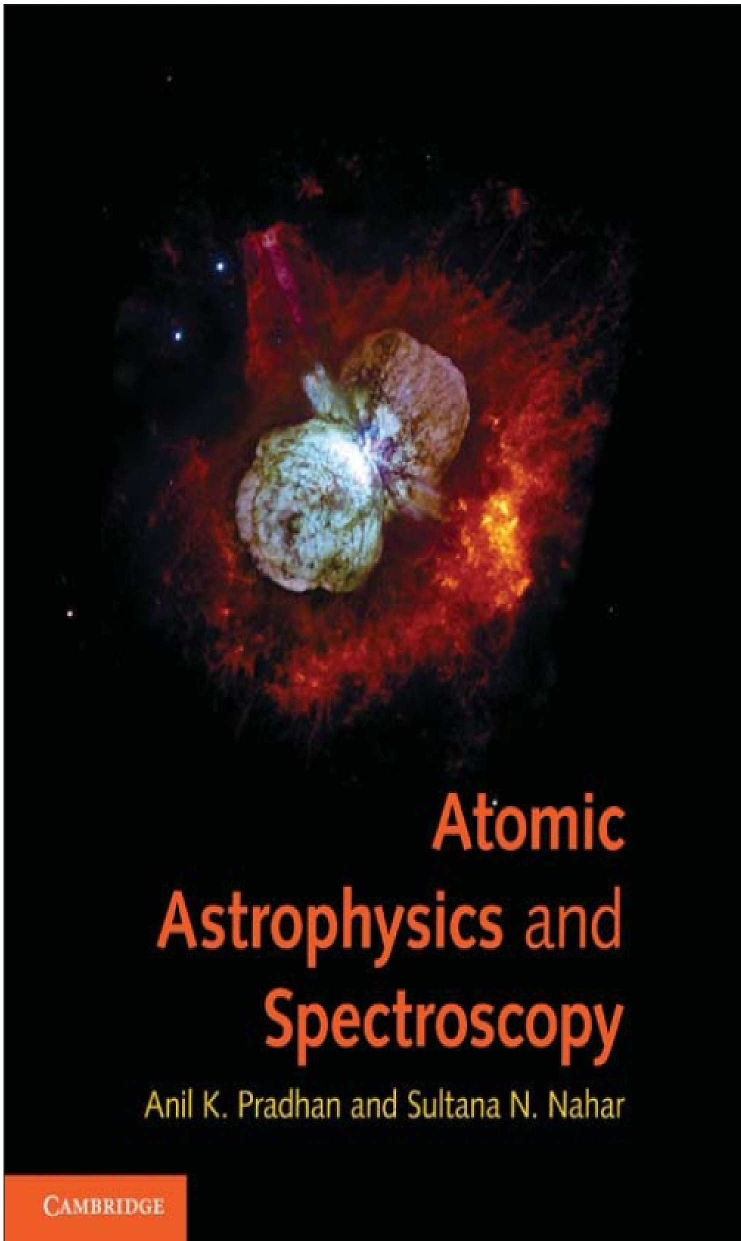

Table of Contents

THEORY:

Breit-Pauli R-matrix (BPRM) Method

Wave Function in Close-Coupling Approximation is an expansion with excited core states:

$$\mathbf{\Psi_E(e + ion) = A \sum_i^N \chi_i(ion)\theta_i + \sum_j c_j\Phi_j(e + ion)}$$

$\chi_\mathbf{i}$ → **Target ion wavefunction,** Φ_j → **correlation functions**
θ_i → **interacting electron wavefunction (continuum or bound)**

- **Resonant Structures - manifested through channel couplings**

- **Table: Levels and energies (E_t) of Ne V in total wave function expansion**
- **Comparison of calculated energies with observed energies in NIST compilation**

	Level	J_t	E_t(Ry) NIST	E_t(Ry) SS
1	$1s^22s^22p^2(^3P)$	0	0.0	0.
2	$1s^22s^22p^2(^3P)$	1	0.003758	0.0030391
3	$1s^22s^22p^2(^3P)$	2	0.010116	0.011366
4	$1s^22s^22p^2(^1D)$	2	0.276036	0.30391
5	$1s^22s^22p^2(^1S)$	2	0.582424	0.57413
6	$1s^22s2p^3(^5S^o)$	2	0.8052	0.71604
7	$1s^22s2p^3(^3D^o)$	3	1.60232	1.62957
8	$1s^22s2p^3(^3D^o)$	2	1.60296	1.62932
9	$1s^22s2p^3(^3D^o)$	1	1.60316	1.62929
10	$1s^22s2p^3(^3P^o)$	2	1.89687	1.92363
11	$1s^22s2p^3(^3P^o)$	1	1.89687	1.92340
12	$1s^22s2p^3(^3P^o)$	0	1.89719	1.92328
13	$1s^22s2p^3(^1D^o)$	2	2.46556	2.59326
14	$1s^22s2p^3(^3S^o)$	1	2.54576	2.64956
15	$1s^22s2p^3(^1P^o)$	1	2.76854	2.88988
16	$1s^22p^4(^3P)$	2	3.76063	3.86076
17	$1s^22p^4(^3P)$	1	3.76778	3.86807
18	$1s^22p^4(^3P)$	0	3.77085	3.87155
19	$1s^22p^4(^1D)$	2		4.13816
20	$1s^22p^4(^1S)$	0		4.74472

Total wave function is obtained solving:

$$\mathbf{H\Psi = E\Psi}$$

R-matrix method is used to solve the Schrodinger eq.

The scattering matrix $\mathbf{S}_{SL\pi}(i,j)$ is obtained from the wave function phase shift. The EIE collision strength is

$$\mathbf{\Omega_{SL\pi} = \frac{1}{2}(2S+1)(2L+1)|S_{SL\pi}(i,j)|^2}$$

The effective collision strength $\mathbf{\Upsilon(T)}$ is the Maxwellian averaged collision strength:

$$\mathbf{\Upsilon(T) = \int_0^\infty \Omega_{ij}(\epsilon_j) e^{-\epsilon_j/kT} d(\epsilon_j/kT)} \qquad (2)$$

The excitation rate coefficient $\mathbf{q_{ij}(T)}$ is

$$\mathbf{q_{ij}(T) = \frac{8.63 \times 10^{-6}}{g_i T^{1/2}} e^{-E_{ij}/kT} \Upsilon(T)\ cm^3 s^{-1}} \qquad (3)$$

ELECTRON IMPACT EXCITATIONS (EIE)

Ne V **Collision strengths Ω(EIE)** (**Dance et al, submitted**):

Top: **Forbidden IR transitions** $2p^2(^3P_0 - ^3P_1)$ **(24**μ**m) and** $2p^2(^3P_1 - ^3P_2)$ **(14**μ**m),**

Bottom: **Forbidden optical transitions** $2p^2(^3P_1 - ^1D_2)$ **(3346Å),** $2p^2(^3P_2 - ^1D_2)$ **(3426Å), and** $2p^2(^1S_0 - ^1D_2)$ **(2973Å)**

- **Resonances at near threshold energy seen for the first time**

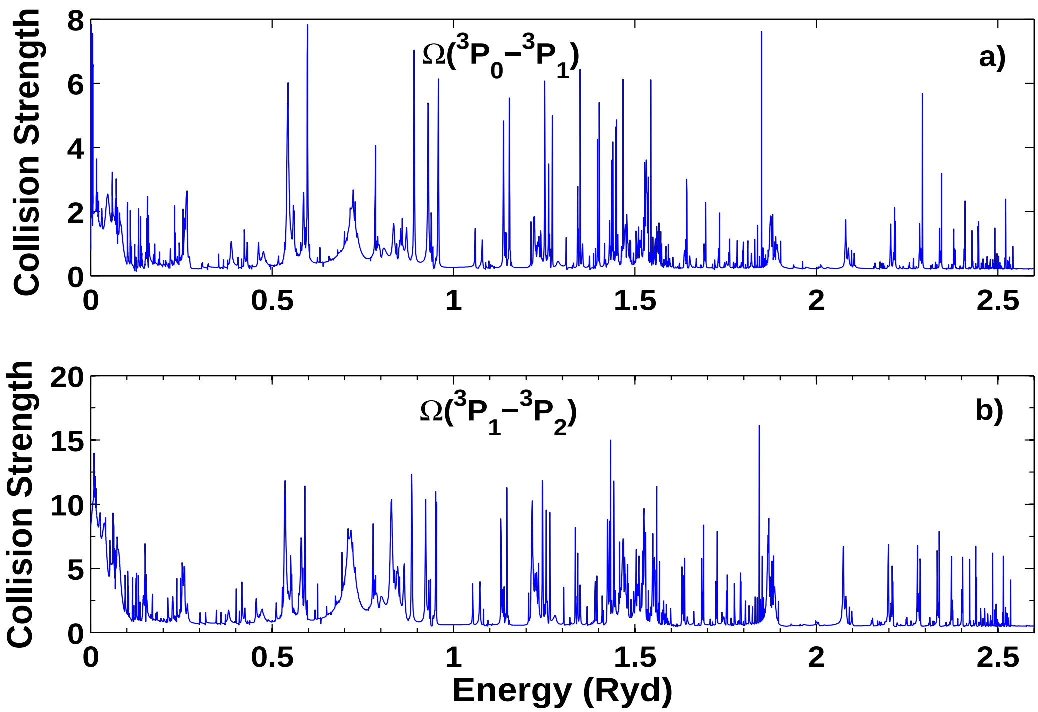

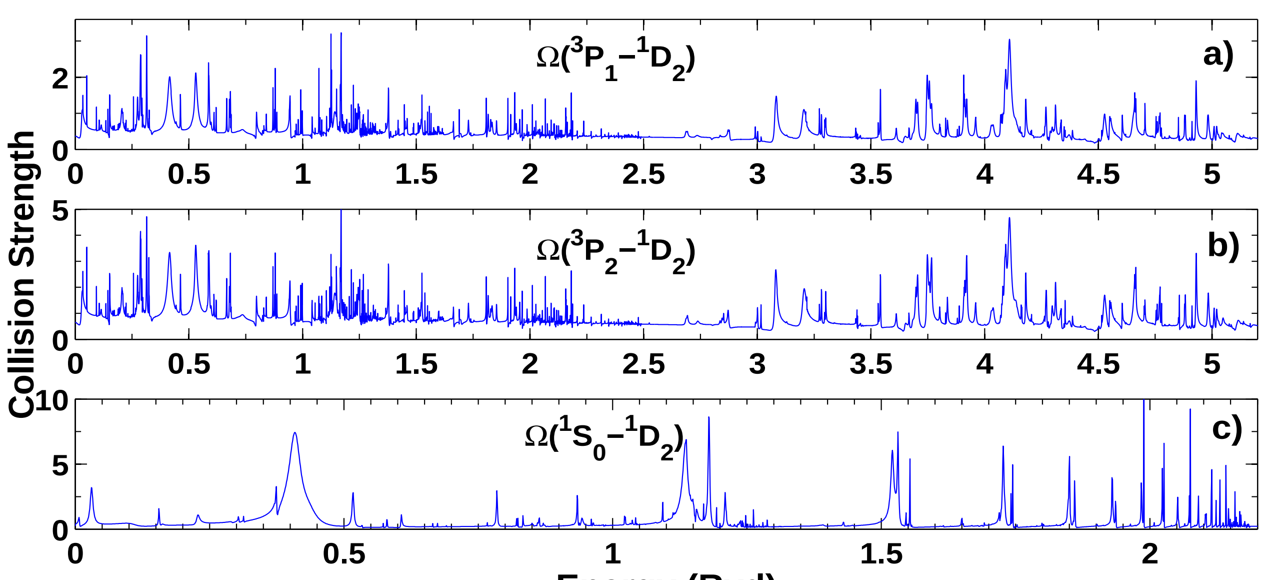

RYDBERG SERIES OF RESONANCES IN EIE

Ne V Collision strengths Ω(EIE) (Dance et al, submitted):

- **Rydberg series of resonances in the near-threshold $\Omega(EIE)$ for $2p^2(^3P_0 - ^3P_1)$ of 24 μm FIR line. Fully resolved at a fine energy mesh of 10^{-6} Ryd**
- **Resonant features not seen before**

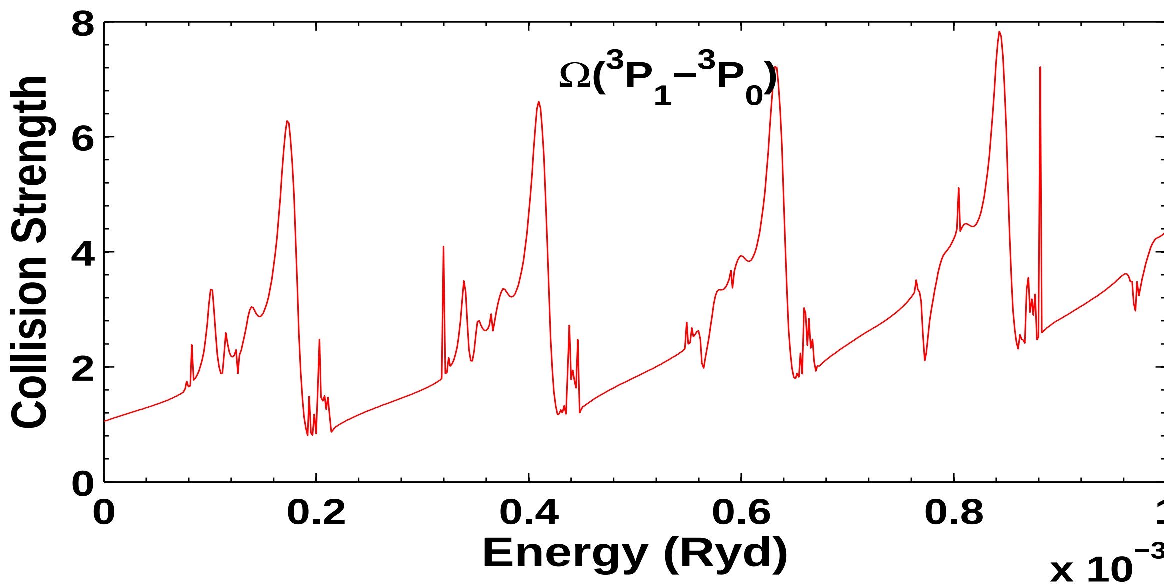

EFFECTIVE COLLISION STRENGTHS: Ne V

Comparison: Effective collision strengths $\Upsilon(T_e)$ (EIE) :

IR: $2p^2(^3P_0 -^3 P_1)$ $(24\mu m)$, $2p^2(^3P_1 -^3 P_2)$ $(14\mu m)$

- Solid curves (present), dotted curves (non-relativistic, Lennon & Burke 1994); dash-dot & dashed curves (BPRM and ICFT, Griffin & Badnell 2000), available at $T_e > 1000$ K
- Present enhancements (IR, 20%, 10%) are due to high resolution resonances at near threshold energy

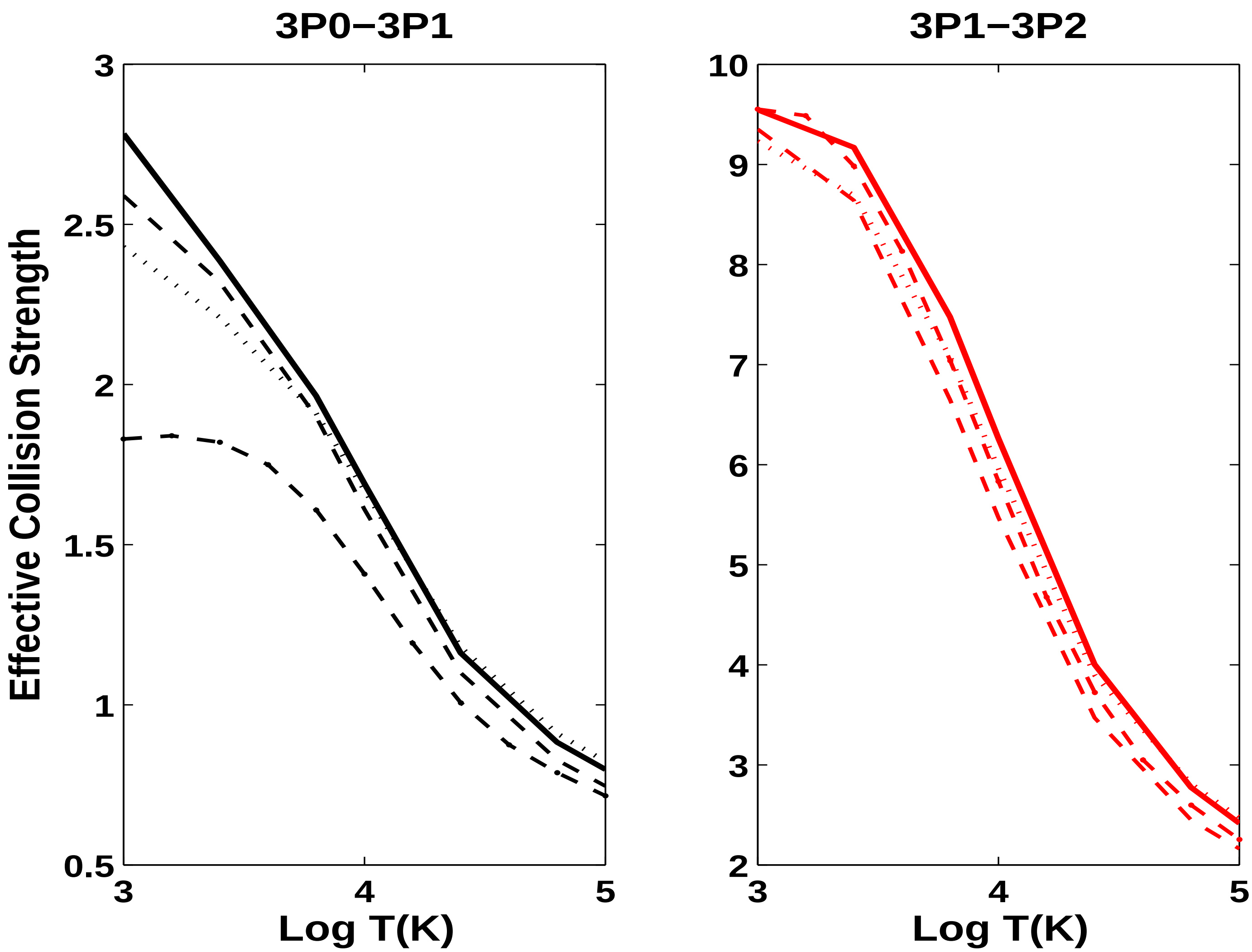

EFFECTIVE COLLISION STRENGTHS: Ne V

Comparison: Effective collision strengths $\Upsilon(T_e)$:

O: $2p^2(^3P_0 -^1 D_2)$ (3301Å), $2p^2(^3P_0 -^1 S_0)$ (1560Å)

- Solid curves (present), dotted curves (non-relativistic, Lennon & Burke 1994); dash-dot & dashed curves (BPRM and ICFT, Griffin & Badnell 2000), available at $T_e > 1000$ K

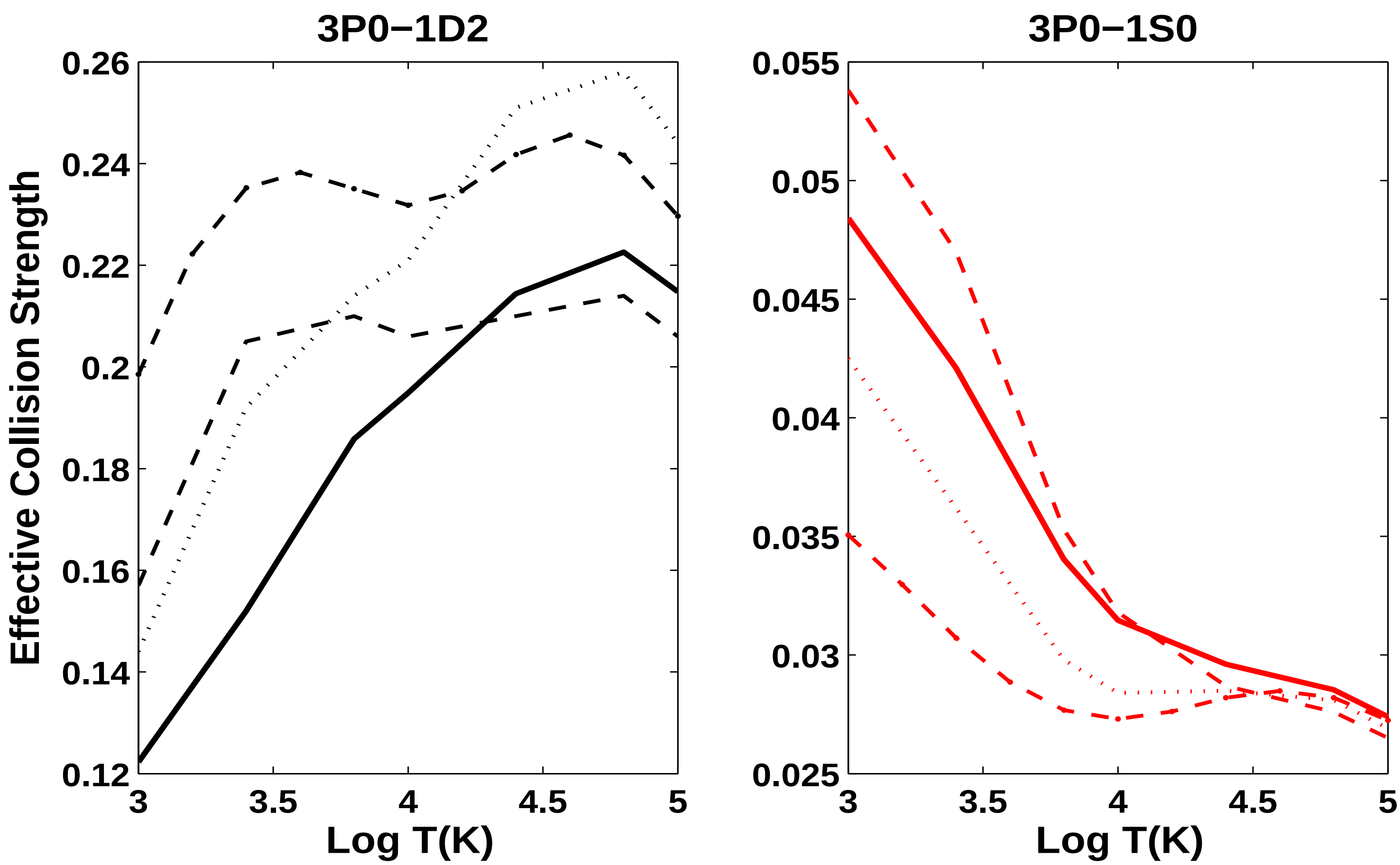

Ne V LINE RATIOS: NEBULAR ρ & T DIAGNOSTICS

• **Comparison:** IR 14/24 μm line emissivity ratios: a) Solid curves (present) at different T, Asterisks (observed from PNe at T = 10,000 K with assigned densities, Rubin 2004), Dotted curves (observed line ratios, outside typical nebular T-ρ range except at low T, Rubin 2004), b) Solid (present), dash (collision stengths, Lennon & Burke 1994)

• Better agreement with observed emissivity ratios at T = 10,000 (10 PNe) and 500 K (anomalously low, 11 PNe)

• Closer agreement due to *systematic* differences in rate coefficients.

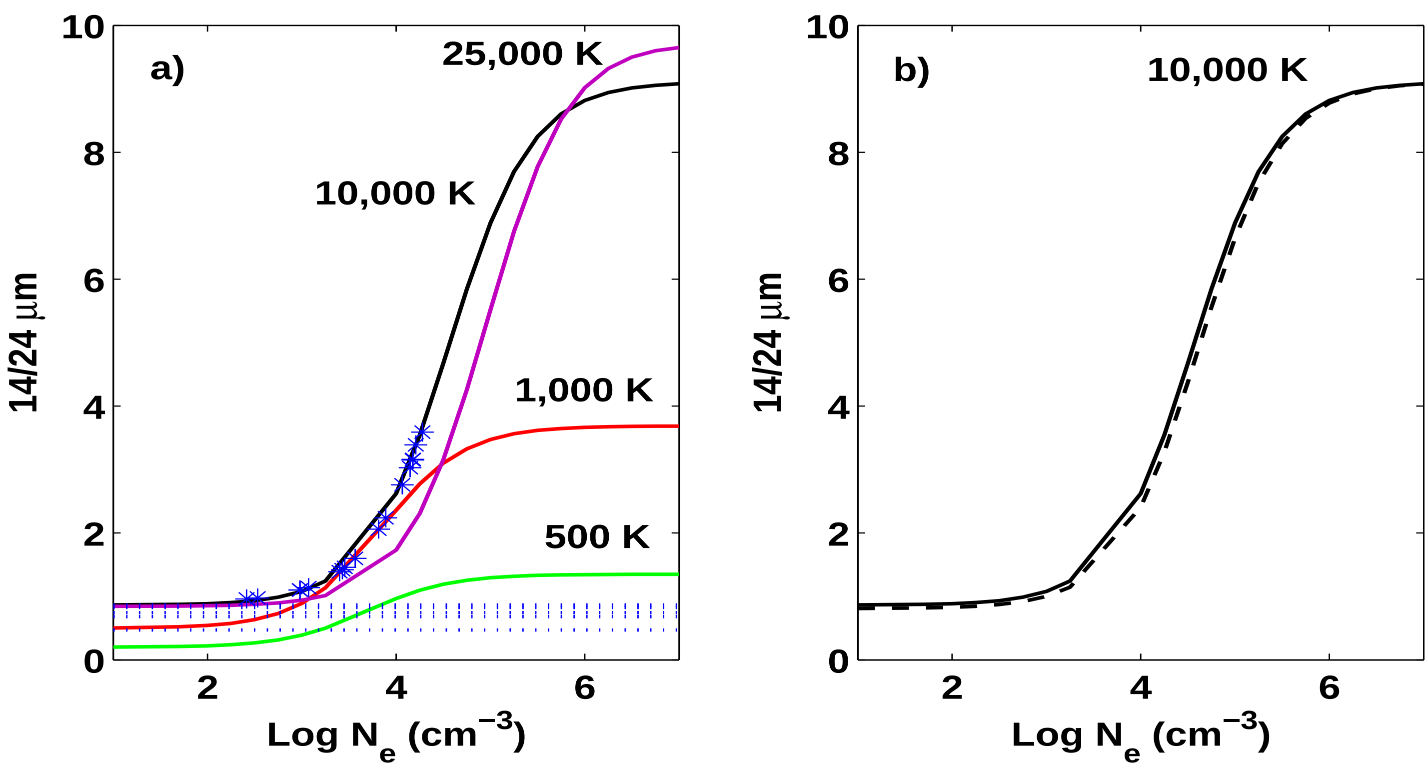

Ne V OPTICAL LINE RATIOS AT NEBULAR ρ & T DIAGNOSTICS

- Comparison: Blended O line ratio (3346+3426)/2973 vs T at $n_e = 10^3$ cm^{-3}
- Closer agreement due to *systematic* differences in rate coefficients.

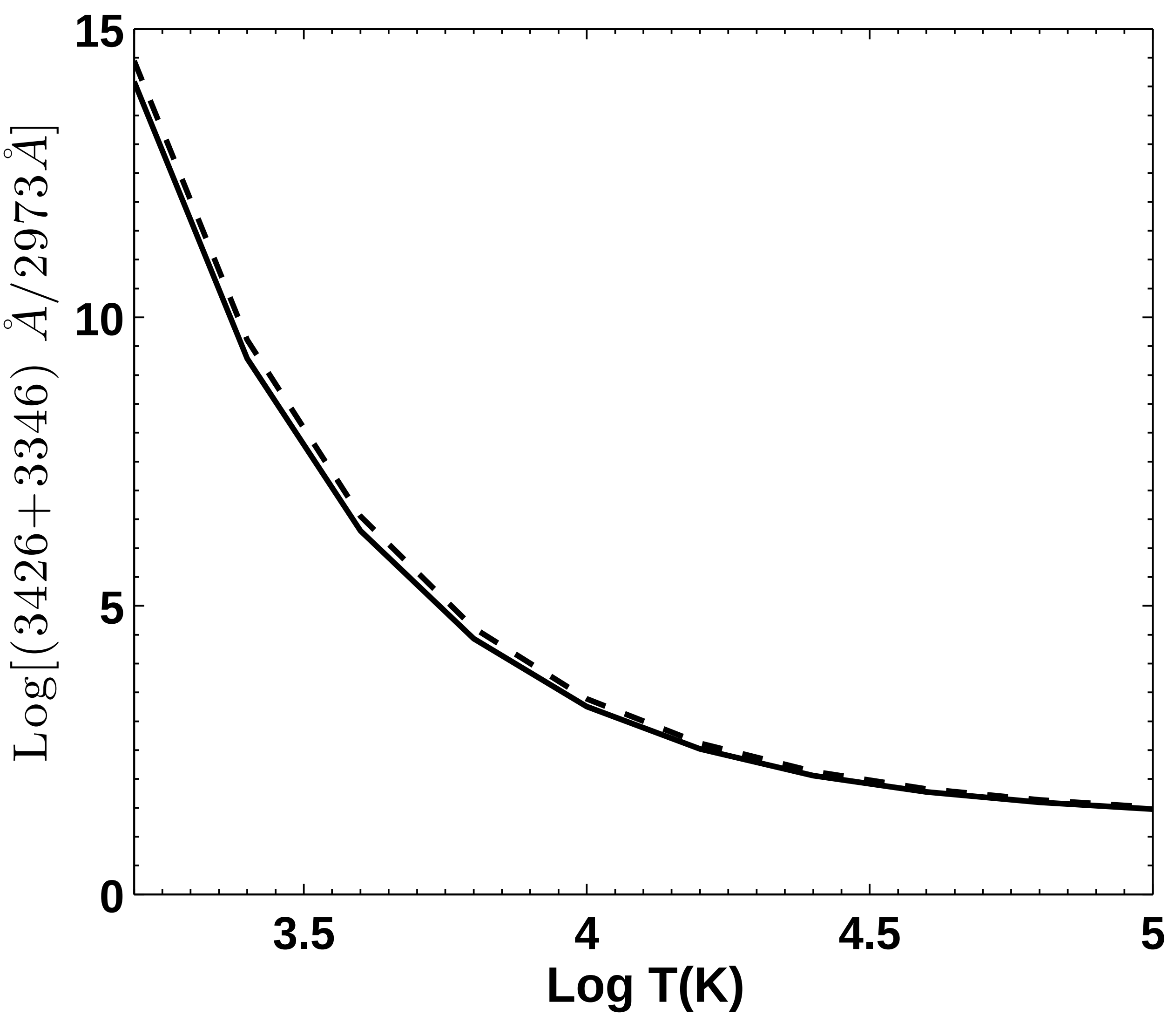

CONCLUSION

1. **We present collision strength and line ratios of forbidden optical and far-infrared transitions in Ne V in nebular temperature and density diagnostics:**
2. **Find prominent resonant features due to fine structure effects in low energy collision cross section not studied before**
3. **A precise delineation of these resonance structures has a significant effect on the mid-IR 14/24 μm line emissivities**
4. **Forbidden optical collision strengths are generally in good agreement with previous works**
5. **New features indicate better agreement with observation, and hence should improve Ne abundance calculations**